Citation: Molecular Therapy — Oncolytics (2016) **3,** 16017; doi:10.1038/mto.2016.17
Official journal of the American Society of Gene & Cell Therapy

www.nature.com/mto

ARTICLE

Systemically administered AAV9-sTRAIL combats invasive glioblastoma in a patient-derived orthotopic xenograft model

Matheus HW Crommentuijn[1,2,3], Rami Kantar[1,2], David P Noske[3], W Peter Vandertop[3], Christian E Badr[1,2], Thomas Würdinger[2,3], Casey A Maguire[1,2] and Bakhos A Tannous[1,2]

Adeno-associated virus (AAV) vectors expressing tumoricidal genes injected directly into brain tumors have shown some promise, however, invasive tumor cells are relatively unaffected. Systemic injection of AAV9 vectors provides widespread delivery to the brain and potentially the tumor/microenvironment. Here we assessed AAV9 for potential glioblastoma therapy using two different promoters driving the expression of the secreted anti-cancer agent sTRAIL as a transgene model; the ubiquitously active chicken β-actin (CBA) promoter and the neuron-specific enolase (NSE) promoter to restrict expression in brain. Intravenous injection of AAV9 vectors encoding a bioluminescent reporter showed similar distribution patterns, although the NSE promoter yielded 100-fold lower expression in the abdomen (liver), with the brain-to-liver expression ratio remaining the same. The main cell types targeted by the CBA promoter were astrocytes, neurons and endothelial cells, while expression by NSE promoter mostly occurred in neurons. Intravenous administration of either AAV9-CBA-sTRAIL or AAV9-NSE-sTRAIL vectors to mice bearing intracranial patient-derived glioblastoma xenografts led to a slower tumor growth and significantly increased survival, with the CBA promoter having higher efficacy. To our knowledge, this is the first report showing the potential of systemic injection of AAV9 vector encoding a therapeutic gene for the treatment of brain tumors.

Molecular Therapy — Oncolytics (2016) **3**, 16017; doi:10.1038/mto.2016.17; published online 22 June 2016

INTRODUCTION

In recent years, adeno-associated virus (AAV) vectors have gained an increasing attention as a gene therapy vector for several diseases, some of which have made it to clinical trials.[1] The first approved AAV-based gene therapy in the Western world is alipogene tiparvovec for the treatment of lipoprotein deficiency, which shows that this approach can be successfully and safely applied to monogenic diseases.[2] Additionally, AAV vectors for the treatment of more complex diseases such as heart failure have seen some success in clinical trials,[3,4] and many advances are made using these vectors as cancer therapeutics.[5]

Glioblastoma (GBM) is the most common and highest-grade malignant primary brain tumor in adults. Despite aggressive therapies, median survival is generally just over one year following diagnosis.[6] This underscores the need for novel treatments to be developed. Tumor necrosis factor-related apoptosis-inducing ligand (TRAIL) is considered as a potent anti-cancer agent, capable of inducing cell death in a variety of tumor cells, including GBM.[7–10] Direct intracranial injection of different AAV vectors into the primary tumor mass have been used for the treatment of GBM (and other brain tumors) with some success, however, due to the invasive nature of this type of cancer, tumor recurrence is typically observed showing that a vector with widespread gene delivery in the brain is required for efficient therapy.[11–13]

AAV9 serotype is very efficient in transducing cells *in vivo*, and has been shown to cross the blood–brain barrier (BBB) upon intravenous injection, making it an ideal candidate for whole brain transduction and potential gene delivery to brain tumors.[14–19] However, AAV9 shows high tropism towards the liver, which may cause off-target toxicity and limit the potential therapeutic effect.[18,20,21] In order to restrict AAV-mediated expression to the brain/tumor environment, a brain cell-specific promoter could be used, such as the neuron-specific enolase (NSE) promoter, which is predominantly active in neurons, thus limiting expression in other cell types/tissues.[22,23] The aim of the current study is to evaluate systemic injection of AAV9 vector expressing a therapeutic gene (secreted soluble TRAIL as a model) under the control of either a constitutively active promoter or neuron-specific promoter for potential therapy of tumors in the brain.

RESULTS

AAV9 transgene expression driven by different promoters has a similar kinetics profile.

We cloned the *Firefly* luciferase bioluminescent reporter under the control of either a constitutively active CBA promoter or neuron-specific NSE promoter and packaged them into AAV9 vector generating AAV9-CBA-Fluc and AAV9-NSE-Fluc (Figure 1a). Athymic nude

The first two authors contributed equally to this work.
[1]Experimental Therapeutics and Molecular Imaging Laboratory, Neuroscience Center, Department of Neurology, Massachusetts General Hospital, Boston, Massachusetts, USA; [2]Program in Neuroscience, Harvard Medical School, Boston, Massachusetts, USA; [3]Neuro-oncology Research Group, Cancer Center Amsterdam, Department of Neurosurgery, VU University Medical Center, Amsterdam, The Netherlands. Correspondence: BA Tannous (btannous@hms.harvard.edu).
Received 5 April 2016; accepted 6 May 2016

mice ($n = 4$ per group) were then injected i.v. via the tail vein with 1.5×10^{12} g.c./kg of each vector and bioluminescence imaging (BLI) was performed at three and twelve days post-injection to quantify the distribution of transgene expression. Widespread delivery of both vectors was observed throughout the animal's body at both time points (Figure 1b). Analysis of the signal from the head and the abdomen of mice at the two time points showed that, at twelve days post administration, AAV9-NSE-Fluc vector yielded an average of 100-fold lower BLI signal in the abdomen ($P = 0.0171$) as well as the brain ($P = 0.0193$) of mice compared to the AAV9-CBA-Fluc vector, indicating that the NSE promoter could be used to decrease transgene expression and potential cytotoxicity in the liver and other tissues (Figure 1b,c). Despite the difference in transgene expression, both vectors yielded a similar expression kinetics profile without significant differences in absolute brain-to-liver expression ratios (Figure 1d). To confirm these results *ex vivo*, mice were sacrificed 20 days postinjection of either vector, and the brain and liver were harvested, homogenized, and analyzed for Fluc expression (normalized to total amount of protein). In line with the expression ratio results obtained by BLI (Figure 1d), an average of 10-fold lower signal in both liver ($P = 0.004$) and the brain (n.s.) was observed with the NSE promoter compared to the CBA promoter (Figure 1e), with no significant differences in the brain-to-liver ratio between both vectors (Figure 1f).

NSE promoter in AAV9 vector transduces mainly neurons in the brain upon i.v. injection

The observed decreased overall expression of the AAV9-NSE-Fluc vector could be due to several factors, including a lower number of cells transduced, expression level per cell, or both. To confirm cell-type selectivity of the NSE promoter, we generated AAV9 vectors expressing GFP under either promoter (AAV9-CBA-GFP and AAV9-NSE-GFP; Figure 2a). These vectors were injected i.v. into nude mice ($n = 3$ per group) at a dose of 5×10^{13} g.c/kg. Two weeks post-vector injection, mice were sacrificed, and the brain and liver were collected, sectioned and stained for GFP expression. In mice injected with AAV9-CBA-GFP, expression of GFP was detected in endothelial cells, neurons and astrocytes in the brain (Figure 2b). On the other hand, and as expected, the most common cell type with GFP expression in the brain of mice injected with AAV9-NSE-GFP were neurons (Figure 2c). In these mice, some dim GFP expression was also observed in endothelial cells while no GFP expression correlated with astrocytes. Furthermore, GFP staining in AAV9-NSE-GFP mice brains coincided mostly with NeuN staining and not with GFAP staining (Supplementary Figure S1), demonstrating that indeed neurons were transduced. Liver sections showed GFP staining, although it was more widespread and intense in sections from mice injected with AAV9-CBA-GFP vector compared to those injected with AAV9-NSE-GFP vector (Figure 2b,c). We also quantified the number of GFP+ cells in three sections and averaged the total number of GFP+ cells per mm^2 showing no significant differences in the number of GFP+ neurons, however significantly more astrocytes ($P < 0.01$) and liver cells ($P < 0.05$) expressed GFP in mice injected with AAV9-CBA-GFP as compared to AAV9-NSE-GFP (Figure 2d).

Intravascular administration of AAV9-sTRAIL vectors inhibits GBM growth in a patient-derived orthotopic xenograft mouse model

In order to assess the potential use of AAV9 vector for systemic delivery of therapeutics to brain tumors, we used the secreted soluble variant of TRAIL as a transgene model and cloned it under the control of NSE or CBA promoter (AAV-CBA-sTRAIL or AAV-NSE-sTRAIL; Figure 3a). Initially, to assess that sTRAIL is secreted in an active form using both constructs, we packaged them into an AAV2 vector and then transduced 293T cells with either vectors or AAV2-NSE-Fluc as a control. Conditioned medium from these cells were collected and used to treat primary GBM neurospheres in triplicate. The AAV-NSE-Fluc control medium had no effect on cell viability. On the other hand, a significantly lower number of viable cells were observed in wells treated with AAV2-CBA-sTRAIL medium, killing 60% of GBM neurospheres as compared to the control group ($P = 0.0008$) as well as in GBM neurospheres treated with AAV2-NSE-sTRAIL medium ($P = 0.0006$; Figure 3b).

We then assessed whether systemic delivery of AAV9-sTRAIL could target the brain tumor environment, while evaluating both CBA and NSE promoters to drive sTRAIL transgene expression, to determine if a restricted promoter also has a similar therapeutic effect *in vivo*. For evaluation of these vectors, we used an invasive patient-derived xenograft orthotopic mouse model.[11,24] Mice were intracranially injected in the left striatum with 2×10^4 of primary GBM stem-like cells culture as neurospheres and expressing *Firefly* luciferase (GBM-Fluc). Twenty-eight days post-tumor cells implantation, mice were pseudo-randomized into treatment groups so that each group had a similar average Fluc signal ($P > 0.9999$; Figure 4 and Supplementary Figure S2) and each group received i.v. injection of 2×10^{13} g.c./kg of either AAV9-CBA-GFP (control, $n = 5$), AAV9-CBA-sTRAIL ($n = 10$) or AAV9-NSE-sTRAIL ($n = 10$). Tumor volume was monitored weekly by Fluc bioluminescence imaging. After the first week post-vector injection, the Fluc signal in the control group had increased significantly, compared to the AAV9-NSE-sTRAIL group ($P = 0.0419$) and compared to the AAV9-CBA-sTRAIL group ($P = 0.0356$), but there was no significant difference between both treatment groups (Figure 4a,b). Between 2 and 3 weeks post-vector injection, all mice in the control group had reached their maximum Fluc tumor signal, after which they were sacrificed due to predetermined humane endpoints. Imaging showed that tumors in both the AAV9-NSE-sTRAIL group and AAV9-CBA-sTRAIL group continued to slowly grow, with the former group showing slightly more growth. However, no significant differences were found at any time point in the Fluc signal between AAV9-NSE-sTRAIL and AAV9-CBA-sTRAIL groups.

Survival analysis showed that there was an overall significant difference between all groups ($P < 0.0001$). *Post-hoc* analysis showed that the survival of control mice was significantly shorter than that of mice treated with AAV9-NSE-sTRAIL ($P = 0.0002$) and those treated with AAV9-CBA-sTRAIL ($P < 0.0001$). This shows that sTRAIL treatment using i.v. administered AAV9 vectors under either promoter provided a therapeutic benefit. Although there was a trend for longer survival in mice treated with AAV9-CBA-sTRAIL as compared to AAV9-NSE-sTRAIL, there was no significant difference between the two vector-treated groups ($P = 0.0998$), despite the fact that Fluc imaging showed a larger tumor size in mice treated with AAV9-NSE-sTRAIL, and that these mice subsequently died sooner. Median survival for the control group was 38 days, while mice treated with AAV9-NSE-sTRAIL or AAV9-CBA-sTRAIL had a median survival of 47 and 54.5 days, respectively (Figure 4c). Furthermore, a small subset of mice ($n = 3$) with AAV9-CBA-sTRAIL survived out to the predetermined end of the study (135 days; Figure 4c). This indicates a trend for longer survival in mice treated with the vector using the CBA promoter over the NSE promoter. To our knowledge, this is the first report showing systemic injection of an AAV vector to treat tumors in the brain.

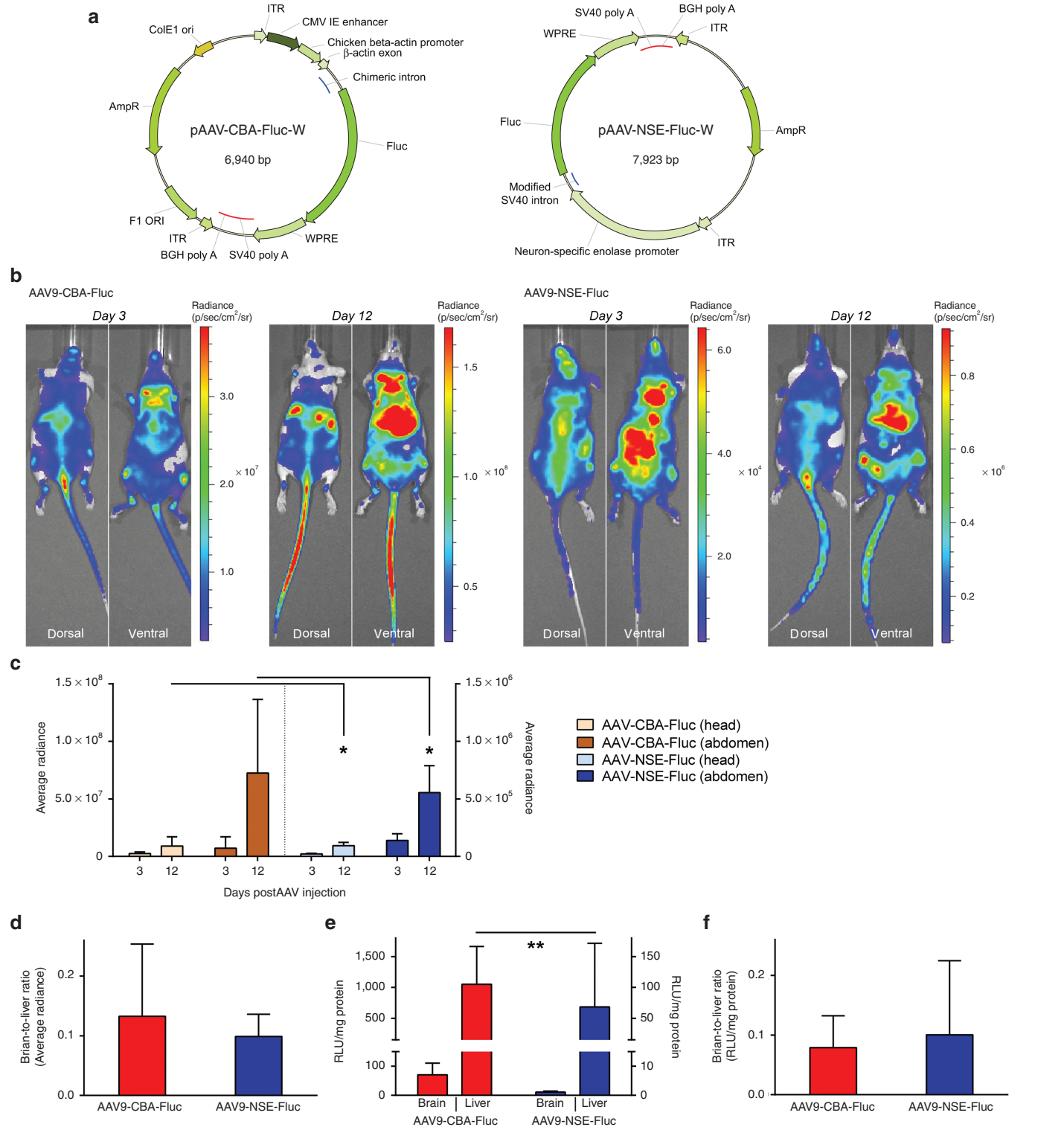

Figure 1 Expression profile and quantitation of adeno-associated virus (AAV)9-mediated bioluminescence expression using chicken β-actin (CBA) or neuron-specific enolase (NSE) promoters. Plasmids were designed for the production of AAV9-CBA-Fluc or AAV9-NSE-Fluc (**a**). Female nude mice ($n = 4$ per group) were injected with 1.5×10^{12} g.c./kg of each vector and images were taken from the dorsal side and ventral side at three and twelve days after administration. A representative mouse at each time point is shown for AAV9-CBA-Fluc (**b**, left panel) and AAV9-NSE-Fluc (**b**, right panel). At 3 and 12 days post vector administration, quantification of the average radiance showed that there is a 100-fold higher signal from the head and abdomen (**c**) in mice injected with AAV9-CBA-Fluc compared to AAV9-NSE-Fluc. No differences in head-to-abdomen ROI ratios were found (**d**). Tissue homogenates showed 10-fold higher relative light units (RLU)/mg in the brain and liver of mice injected with AAV9-CBA-Fluc compared to AAV9-NSE-Fluc (**e**), with no significant differences in the brain-to-liver tissue homogenate ratios (**f**). Note the scale difference between left and right axis in **c** and **e** (*$P < 0.05$; **$P < 0.005$).

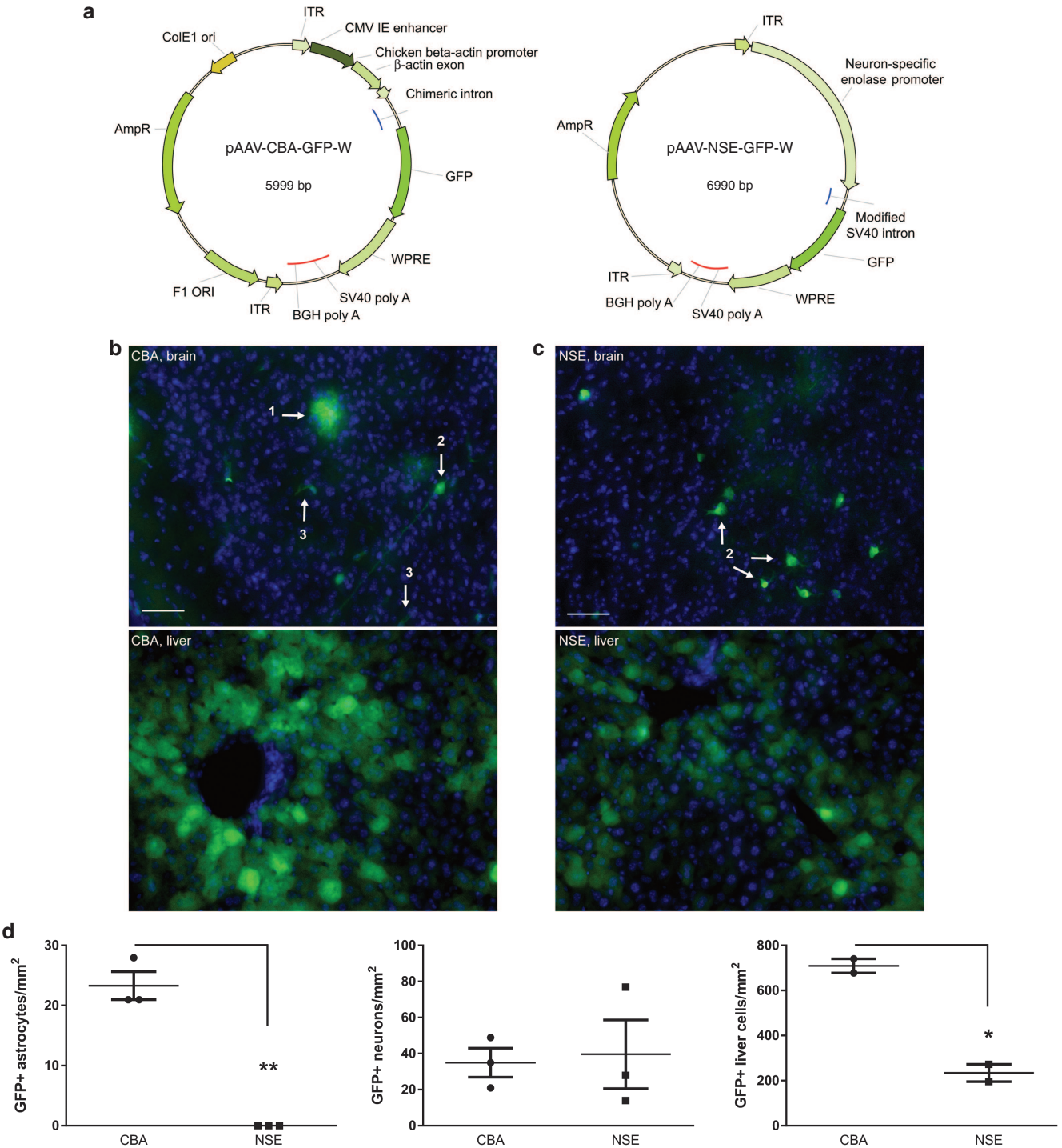

Figure 2 Brain cell specificity and liver expression with AAV9-CBA-GFP or AAV9-NSE-GFP vector. Mice were injected i.v. with 5×10^{13} g.c./kg of AAV9-CBA-GFP or AAV9-NSE-GFP vector (**a**), perfused 2 weeks later and brains and livers were harvested and stained for GFP. In the brains of mice injected with AAV9-CBA-GFP (**b**, top panel), astrocytes (1), neurons (2) and endothelial cells (3) clearly expressed GFP, while primarily neurons (2) expressed GFP in brains of mice injected with AAV9-NSE-GFP (**c**, top panel). Both vectors efficiently transduced neurons and expressed GFP. Expression of GFP was also detected in the liver, with higher expression in the livers of mice injected with AAV9-CBA-GFP (**b**, lower panel) than AAV9-NSE-GFP (**c**, lower panel). Scale bar: 50 µm. Quantitation of GFP+ cells was averaged over three sections and the number of GFP+ cells per mm^2 was calculated and plotted (**d**) (*$P < 0.05$; **$P < 0.01$).

Next, we performed *ex vivo* histological analysis using H&E staining and Ki-67 staining for cell proliferation on brains of mice sacrificed at 6 weeks post-tumor inoculation. In addition, as TRAIL might induce hepatotoxicity and AAV9 is known to efficiently transduce cells in the liver, we also performed H&E staining on liver sections to establish whether this therapy caused any histopathological changes. Gross histological analysis did not reveal any visible differences in liver sections across the different groups (Supplementary Figure S3). Large tumors were found at the injection site in the brains of mice from the control group. In contrast, much fewer tumor cells

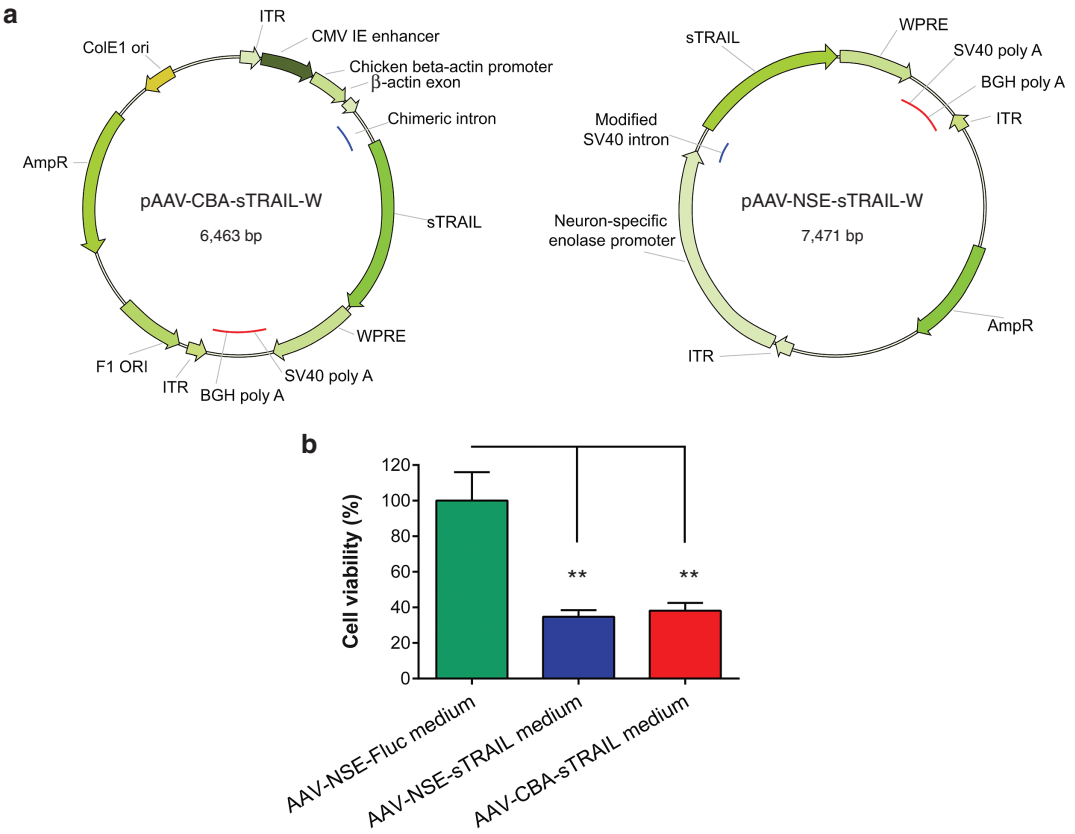

Figure 3 Cells transduced with AAV-CBA-sTRAIL or AAV-NSE-sTRAIL secrete TRAIL in an active form. 293T cells were transduced with either AAV2-CBA-sTRAIL, AAV2-NSE-sTRAIL (**a**) or AAV2-NSE-Fluc control vector. Three days later, conditioned medium was transferred to wells containing GBM neurospheres, and the next day cell viability was measured (**b**). GBM cell viability decreased significantly in wells treated with AAV2-CBA-sTRAIL or AAV2-NSE-sTRAIL compared to control wells (**$P < 0.001$).

were visible on H&E stained sections of mice brains in the AAV9-NSE-sTRAIL or AAV9-CBA-sTRAIL groups (Figure 4d). Ki-67 staining often matched H&E staining and was observed around tumor sites in all brain sections, indicating actively proliferating cells (Figure 4d).

DISCUSSION

The use of AAV as a preclinical gene therapy delivery vector has resulted in significant successes.[1] The ability of AAV9 to efficiently pass the BBB after intravascular (i.v.) administration makes this serotype uniquely suited for gene therapy of the CNS, particularly the brain.[16,18] GBM is an aggressive form of primary brain cancer that is notoriously resistant to therapies. The presence of death signaling receptors on the membrane of GBM cells makes their ligand, TRAIL, a potential therapy. Unfortunately, the short half-life and its inability to cross the blood–brain barrier are a major problem when using recombinant TRAIL protein for therapy in the brain.[25,26] AAV vectors encoding TRAIL have been utilized for the treatment of many forms of cancer, although most studies use intratumoral or near-tumor administration[27–29] rather than systemic administration.[30,31] In case of the brain, systemic delivery is hampered due to limited BBB penetration and subsequent poor brain distribution of many AAV vectors and TRAIL protein.[11,21,25] Here we used i.v.-administered AAV9 vectors for delivery of sTRAIL (as a transgene model) to the primary tumor mass and infiltrating tumor cells in the brain. Although TRAIL's proapoptotic effects are confined to tumor cells,[32–34] high levels of TRAIL or other transgene expression in the liver[21,35] become a concern leading to toxicity.[36,37] To overcome potential liver toxicity, we used the neuron-specific enolase (NSE) promoter, predominantly active in neurons,[22] and compared it to the ubiquitously active chicken beta-actin (CBA) promoter. Our data show that the NSE promoter reduced transgene expression in the brain and the liver by at least 10-fold compared to the CBA promoter, although the brain-to-liver ratio remained the same. This is likely due to the fact that in adult mice, AAV9 primarily transduces astrocytes.[17] By restricting expression to mostly neurons in the brain, we likely lowered the overall transgene expression levels in the brain. Indeed, we observed that while the CBA promoter leads to expression in most cell types in the brain, most notably neurons, astrocytes and endothelial cells, the NSE promoter leads to a more confined expression in neurons with low expression in endothelial cells and much less expression in the liver. Further, the NSE promoter may also be weaker on a per neuron basis than the CBA promoter, in line with other studies.[38,39] In the future, we may be able to maintain high expression of transgene in the brain and lower expression in the liver by employing miR122 target sites into the 3'UTR of the transgene cassette as previously described.[40]

We have previously shown that intracranially administered AAVrh.8-sTRAIL was capable of combating primary GBM tumor mass in a nude mouse model, however, single vector injection was not able to combat invasive cells, which managed to escape the zone of resistance and form a new tumor elsewhere in the mouse brain leading to tumor recurrence.[11] In addition to intracranial injections being a laborious procedure, i.v. administration of a therapeutic vector with widespread CNS transduction would be advantageous since it could target both the primary tumor mass as well as infiltrative tumor cells in the brain. Indeed, a single i.v. injection of either AAV9-CBA-sTRAIL or AAV9-NSE-sTRAIL vectors lead to a significantly slower tumor growth

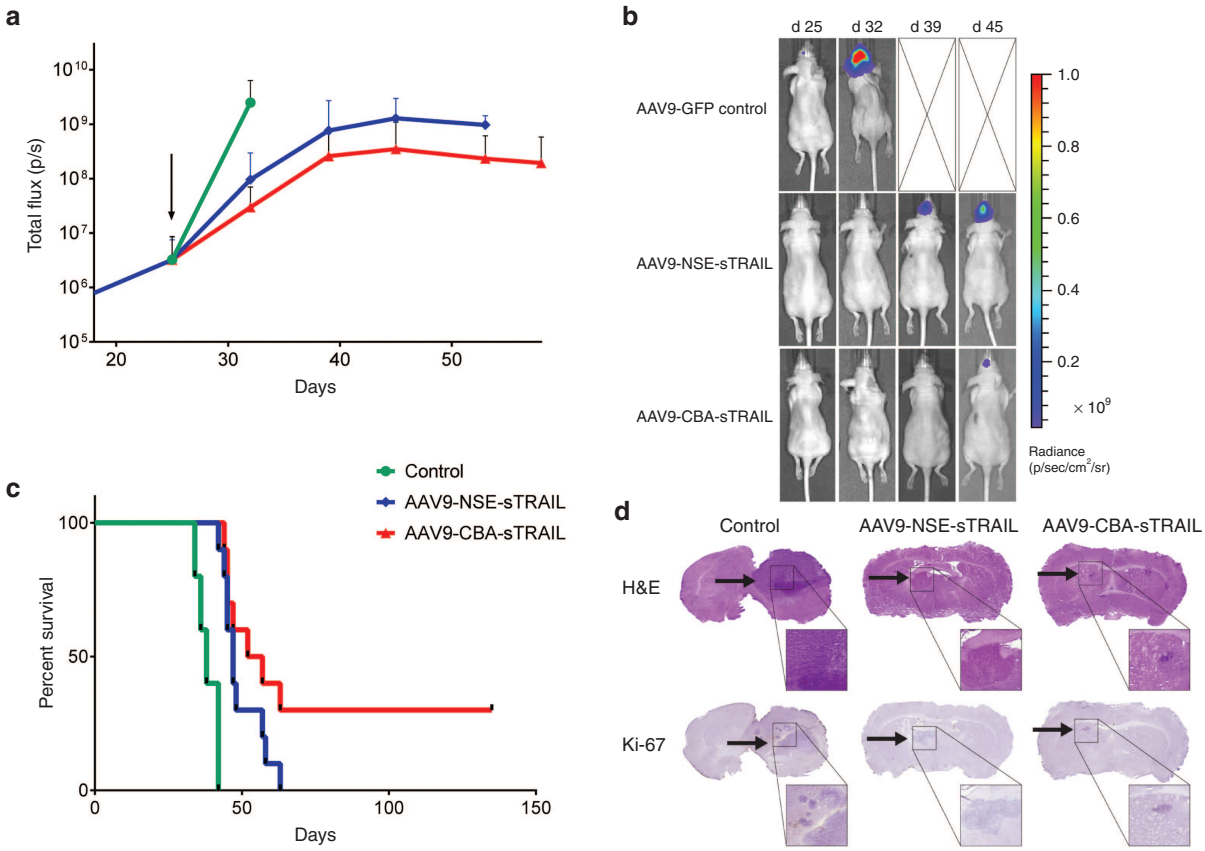

Figure 4 Systemic delivery of AAV9-sTRAIL slows invasive GBM tumor growth in the brain. Mice were intracranially injected with patient-derived GBM stem-like neurospheres expressing Fluc (GBM-Fluc). Twenty-eight days later, mice were randomized into three groups, which were i.v. injected with 2×10^{13} g.c./kg of either AAV9-GFP control, AAV9-NSE-sTRAIL or AAV9-CBA-sTRAIL. (**a**) Weekly bioluminescence imaging was used to monitor tumor response. Arrow indicates the start of the treatment. (**b**) A representative bioluminescence image of a single mouse from each group is shown at different time points. (**c**) Kaplan-Meier survival curves for the three different treatment groups. (**d**) H&E and Ki-67 staining of brain sections. A representative section of a mouse from each group is shown at six weeks post-tumor inoculation.

and increase in survival rate as compared to mice treated with AAV9-CBA-GFP control vector. Although there was a general trend in slower tumor growth and increase in survival of mice treated with AAV9-CBA-sTRAIL as compared to AAV9-NSE-sTRAIL vector, there were no significant differences between both groups showing the efficacy of neuron-specific promoter with lower liver transduction in combating aggressive GBM cells. To our knowledge, this is the first report showing that systemic injection of an AAV vector could treat tumors in the brain using a brain-specific promoter with lower liver expression.

Massive invasion of the brain is a major problem in controlling GBM growth. Unfortunately, this therapy did not sufficiently inhibit the spread of GBM cells to other parts of the brain, away from the primary tumor site and eventually all mice died. Additionally, resistance to therapy (including TRAIL) is a major problem for the treatment of GBM.[41–43] We initially tried a relatively low dose of AAV9-sTRAIL (2×10^{13} g.c./kg). A higher dose of AAV9-sTRAIL or multiple rounds of therapy, combined with TRAIL-sensitizing agents,[44–47] may achieve a greater benefit for inhibiting the invasive growth of GBM and prevent intrinsic or acquired TRAIL resistance. TRAIL did not appear to have affected the liver, as there was no indication of liver toxicity in both AAV-sTRAIL-treated groups as observed in the H&E stained sections. Therefore, promoter restriction might not be necessary for limiting TRAIL expression in non-target tissues such as the liver (at least in mice). However, restricting transgene expression of TRAIL from liver could still be a concern due to cell-mediated immunity against AAV capsid or the transgene,[35,48] especially in patients with underlying liver pathologies.[49]

In conclusion, systemically-delivered AAV9 encoding a therapeutic protein is a promising approach to GBM therapy. Future experiments using higher vector doses, different transgene expression cassettes, combined with TRAIL-sensitizing compounds should lead to a more pronounced survival benefit.

MATERIALS AND METHODS

Cloning

The pAAV-NSE-Fluc vector was constructed by digesting pAAV-NSE-GFP[50] and pAAV-CBA-Fluc[51] with NheI and SacI (New England Biolabs, Ipswich, MA), replacing GFP with Fluc. The pAAV-CBA-sTRAIL vector has been previously described.[52,53] From this vector, sTRAIL was amplified by polymerase chain reaction (PCR) using the following primers: AgeI forward 5′-GACACCGGTGACGCCGCCACCATGACAG-3′ and SpeI reverse 5′-GGACTAGTTTAGCCAACTAAAAAGGCCCCGAA-3′. After digesting sTRAIL with AgeI and SpeI, respective inserts were ligated into a similarly digested pAAV-NSE-GFP, generating pAAV-NSE-sTRAIL.

Cell culture and viral vector production

293T cells, for AAV production, obtained from American Type Culture Collection (ATCC, Manassas, VA) were cultured in high-glucose Dulbecco's modified eagle medium (DMEM; Invitrogen, Carlsbad, CA) supplemented with 10% fetal bovine serum (FBS; Sigma, St. Louis, MO), 100 U of penicillin/0.1 mg/ml streptomycin complex (Pen/Strep; Invitrogen, Carlsbad, CA). Primary stem-like GBM8 glioblastoma cells[24] were cultured as neurospheres in serum-free NeuroCult NS-A Basal Medium with Proliferation Supplement (StemCell Technologies, Vancouver, BC), supplemented with 20 ng/ml recombinant epidermal growth factor (EGF; R&D Systems, Minneapolis, MN), 10 ng/ml basic fibroblast growth factor (bFGF; Peprotech, Rocky Hill, NJ),

and 2 µg/ml heparin (Sigma). All cells were cultured at 37 °C under 5% CO_2 humidified atmosphere.

AAV vectors were produced as previously described.[54] Briefly, triple transfection of 293T cells using calcium phosphate precipitation was used with AAV2 ITR-containing single-stranded transgene plasmid, mini-adenovirus helper plasmid pFD6, and pH22 (AAV2 capsid; for *in vitro* use) or pAR9 (AAV9 capsid; for *in vivo* use) rep/cap plasmid. Three days later, the cells were harvested, lysed by freeze/thaw, and AAV was purified using iodixanol density gradient ultracentrifugation, resulting in typical yields of 10^{13} genome copies per ml (g.c./ml).

Cell viability assay

For production of sTRAIL protein, 4×10^5 293T cells per well were plated in a 12-well plate. The next day, cells were transduced with 1×10^4 g.c./cell AAV2-NSE-Fluc (control), AAV2-NSE-sTRAIL, or AAV2-CBA-sTRAIL. We have previously shown that the NSE promoter is active in 293T cells.[50] The day after 293T cell transduction, 5×10^3 GBM8 cells were plated in each well of a 96-well plate. Two days later, conditioned medium from 293T producer cells was harvested and added to the GBM8 cells for all conditions in triplicate. Twenty-four hours after treatment, quantification of cell viability and ATP detection in metabolically active cells was performed using the commercially available CellTiter-Glo assay as per manufacturer's protocol (Promega, Madison, WI). Readout of relative light units (RLUs) was performed using a luminometer (Dynex Technologies, Chantilly, VA) and control samples were used to assess background signal in the medium and cell viability in each treatment group. After subtraction of background, the mean RLU per group was plotted as a percentage, with the control group set at 100%.

GBM animal models and bioluminescence imaging

All animal experiments were approved by the Massachusetts General Hospital (MGH) subcommittee on Research Animal Care and performed according to their guidelines and regulations. Female athymic nude mice of 6–8 weeks old, weighing 20–25 g, were obtained from MGH research animal services, and housed at their animal facility. For tail vein injections, each mouse was placed in a restrainer (Braintree Scientific, Braintree, MA); the tail was warmed up in a beaker with water at 40 °C and swabbed with alcohol. Mice were injected i.v. with a 200 µl mixture of PBS containing 1.5×10^{12} g.c./kg of either AAV9-CBA-Fluc or AAV9-NSE-Fluc vector, or 5×10^{13} g.c./kg of AAV9-CBA-GFP or AAV9-NSE-GFP vector, or 2×10^{13} g.c./kg of AAV9-CBA-sTRAIL or AAV9-NSE-sTRAIL vector.

To generate GBM models, mice were anesthetized with a mixture of 100 mg/kg ketamine and 5 mg/kg xylazine in 0.9% sterile saline. Mice were placed in a stereotaxic frame and intracranially injected with 2×10^4 GBM8-Fluc cells using a Micro 4 Microsyringe Pump Controller (World Precision Instruments, Sarasota, FL) attached to a Hamilton syringe with a 33-gauge needle (Hamilton, Reno, NV), at the following coordinates in mm from bregma: +0.5 antero-posterior, +2.0 medio-lateral, -2.5 dorso-ventral.

To assess the transduction efficiency of AAV9-Fluc vectors or GBM8-Fluc tumor growth, Fluc expression in mice was imaged noninvasively using a Xenogen IVIS Spectrum charge-coupled device (CCD) camera (Caliper Life Sciences, Hopkinton, MA), equipped with an XGI-8 gas anesthesia system. Mice were anesthetized with 2.5% isoflurane in oxygen and the Fluc signal was acquired 10 minutes after i.p. injection of 200 mg/kg $_D$-luciferin (Gold Biotechnology, St. Louis, MO) using the auto-exposure function. For AAV9-Fluc vectors, the dorsal and ventral sides of mice were imaged for Fluc expression. The Living Image software package was used to draw a region of interest (ROI) around the abdomen or the head of mice and to quantify intensity of luminescent signal.

Tissue homogenates

Twenty days after AAV9-Fluc vector injections ($n = 4$ per group), mice were anesthetized and sacrificed by i.p. injection with an overdose mixture of ketamine (300 mg/kg) and xylazine (15 mg/kg) in sterile 0.9% saline. Liver and brain were harvested, snap frozen on liquid nitrogen and stored at −80 °C. For *ex vivo* assays, 50 mg of each tissue was lysed in a 96-deepwell plate (Nunc/Thermo Fisher Scientific, Waltham, MA) by adding a stainless steel bead (Qiagen, Valencia, CA) and 500 µl of Mammalian Protein Extraction Reagent (M-PER; Pierce Biotechnology, Rockford, IL) and homogenized using the TissueLyser II (Qiagen) at 7.0 Hz for four times 3 minutes. The adapter holding the plate was inversed each time to ensure proper lysing. Next, the plate was centrifuged for 5 minutes at 1,200 rpm. The Bradford assay (Bio-Rad Labs, Hercules, CA) was performed according to manufacturer's protocol to quantify protein amounts in each sample. Each homogenized sample was diluted 1 to 50 in order to be in the linear range of the microplate standard assay. For the Fluc assay, 20 µl of each homogenized tissue was transferred to a 96-well white bottom place. The luminometer (Dynex Technologies, Chantilly, VA) was programmed to add 100 µl of Bright-Glo Fluc substrate reagent (Promega, Madison, WI) to each well and analyze the signal during a ten-second integrated reading. Individual values of milligram protein and Fluc RLU for each tissue sample were obtained. After subtraction of background, the RLU/mg protein was calculated for matched samples.

Fluorescence, histology, and immunohistochemistry

Fifteen days post-i.v. injection of 5×10^{13} g.c./kg AAV9-CBA-GFP or AAV9-NSE-GFP ($n = 3$ per group), mice were anesthetized and transcardially perfused with PBS for 3 minutes to flush out the blood, followed by 4% paraformaldehyde (PFA; Affymetrix/USB Products, Santa Clara, CA) for 7 minutes to fix tissues. The brain and liver from each mouse were harvested, postfixed for 24–48 hours in 4% PFA at 4 °C and then transferred to 30% sucrose in PBS for 48–72 hours at 4 °C for cryoprotection. Tissues were embedded in Neg-50 frozen section medium (Fisher Scientific, Pittsburgh, PA) using a dry ice/2-ethylbutanol bath and mounted in a Microm HM550 cryostat (Thermo Scientific, Kalamazoo, MI). Throughout the entire brain or liver, one-in-five 40 µm-thick coronal sections were collected in two (liver) or three (brain) consecutive series, transferred to a 24-well plate containing PBS kept on ice, and stored at 4 °C. Immunofluorescence was performed on free-floating sections. The sections were permeabilized using 0.5% Triton X-100 in PBS and nonspecific binding was blocked with 5% normal goat serum (NGS) in PBS. Primary antibody specific for GFP (rabbit anti-GFP, ABfinity, 1:400; Life Technologies, Carlsbad, CA) was diluted in 1.5% NGS in PBS and incubated for 60 hours at 4 °C in stirring condition. Next, 1:1,000 diluted secondary antibody (goat anti-rabbit Alexa Fluor 488, Cell Signaling, Danvers, MA) was incubated for 1 hour at room temperature in stirring condition. Nucleic staining was performed with DAPI, and, after final washes in PBS, sections were carefully mounted onto slides using a brush and dried overnight. Finally, fluorescence mounting medium (Dako North America, Carpinteria, CA) was applied and sections were covered with a coverslip. Once the mounting medium dried, slides were viewed under a Zeiss AxioObserver Z1 fluorescence microscope (Carl Zeiss Microscopy, Thornwood, NY) with an automated stage for capturing images using the Zen software package (Carl Zeiss Microscopy, Thornwood, NY). Cell type was determined based on morphology. The number of GFP+ cells for each cell type was counted per section and then averaged over the total area in mm^2.

Statistics

Statistical analysis was performed using GraphPad Prism (v6.01; LaJolla, CA). A P value ≤ 0.05 was considered statistically significant. To compare promoter differences between tissues or between days, a two-way analysis of variance was used followed by a Sidak Multiple Comparison test to compare individual groups. Otherwise, comparisons between two samples were analyzed using an unpaired two-tailed t-test. For analysis between multiple groups, a one-way analysis of variance was performed, again followed by a Sidak Multiple Comparison Test. Survival was analyzed using Kaplan-Meier curves and log-rank (Mantel-Cox) tests to compare all or individual groups.

ACKNOWLEDGMENTS

This study was supported by grants from the National Institutes of Health (NIH), the National Institute of Neurological Disorders and Stroke (NINDS) R01NS064983 (B.A.T.) and the American Brain Tumor Association Discovery Grant (C.A.M.). The authors acknowledge the support from 1S10RR025504 Shared Instrumentation Grant IVIS imaging system that was used to acquire imaging data. M.H.W.C. was supported by a scholarship from KWF Kankerbestrijding (Dutch Cancer Society). The authors would like to thank Kevin Conway for the production of lentivirus vectors at the MGH Vector Core, Charlestown, MA, USA (supported by NIH/NINDS P30NS045776; BAT).

REFERENCES

1. Kotterman, MA and Schaffer, DV (2014). Engineering adeno-associated viruses for clinical gene therapy. *Nat Rev Genet* **15**: 445–451.
2. Salmon, F, Grosios, K and Petry, H (2014). Safety profile of recombinant adeno-associated viral vectors: focus on alipogene tiparvovec (Glybera®). *Expert Rev Clin Pharmacol* **7**: 53–65.
3. Hayward, C, Patel, H and Lyon, A (2014). Gene therapy in heart failure. SERCA2a as a therapeutic target. *Circ J* **78**: 2577–2587.
4. Zsebo, K, Yaroshinsky, A, Rudy, JJ, Wagner, K, Greenberg, B, Jessup, M *et al.* (2014). Long-term effects of AAV1/SERCA2a gene transfer in patients with severe heart failure: analysis of recurrent cardiovascular events and mortality. *Circ Res* **114**: 101–108.
5. Luo, J, Luo, Y, Sun, J, Zhou, Y, Zhang, Y and Yang, X (2015). Adeno-associated virus-mediated cancer gene therapy: current status. *Cancer Lett* **356**(2 Pt B): 347–356.
6. Stupp, R, Mason, WP, van den Bent, MJ, Weller, M, Fisher, B, Taphoorn, MJ *et al.*; European Organisation for Research and Treatment of Cancer Brain Tumor and Radiotherapy

Groups; National Cancer Institute of Canada Clinical Trials Group. (2005). Radiotherapy plus concomitant and adjuvant temozolomide for glioblastoma. *N Engl J Med* **352**: 987–996.
7. Song, JH, Song, DK, Pyrzynska, B, Petruk, KC, Van Meir, EG and Hao, C (2003). TRAIL triggers apoptosis in human malignant glioma cells through extrinsic and intrinsic pathways. *Brain Pathol* **13**: 539–553.
8. Bouralexis, S, Findlay, DM and Evdokiou, A (2005). Death to the bad guys: targeting cancer via Apo2L/TRAIL. *Apoptosis* **10**: 35–51.
9. Kuijlen, JM, Bremer, E, Mooij, JJ, den Dunnen, WF and Helfrich, W (2010). Review: on TRAIL for malignant glioma therapy? *Neuropathol Appl Neurobiol* **36**: 168–182.
10. Chiu, TL, Wang, MJ and Su, CC (2012). The treatment of glioblastoma multiforme through activation of microglia and TRAIL induced by rAAV2-mediated IL-12 in a syngeneic rat model. *J Biomed Sci* **19**: 45.
11. Crommentuijn, MH, Maguire, CA, Niers, JM, Vandertop, WP, Badr, CE, Würdinger, T *et al.* (2016). Intracranial AAV-sTRAIL combined with lanatoside C prolongs survival in an orthotopic xenograft mouse model of invasive glioblastoma. *Mol Oncol* **10**: 625–634.
12. Ma, HI, Hueng, DY, Shui, HA, Han, JM, Wang, CH, Lai, YH *et al.* (2014). Intratumoral decorin gene delivery by AAV vector inhibits brain glioblastomas and prolongs survival of animals by inducing cell differentiation. *Int J Mol Sci* **15**: 4393–4414.
13. Hicks, MJ, Funato, K, Wang, L, Aronowitz, E, Dyke, JP, Ballon, DJ *et al.* (2015). Genetic modification of neurons to express bevacizumab for local anti-angiogenesis treatment of glioblastoma. *Cancer Gene Ther* **22**: 1–8.
14. Gao, G, Vandenberghe, LH, Alvira, MR, Lu, Y, Calcedo, R, Zhou, X *et al.* (2004). Clades of Adeno-associated viruses are widely disseminated in human tissues. *J Virol* **78**: 6381–6388.
15. Bish, LT, Morine, K, Sleeper, MM, Sanmiguel, J, Wu, D, Gao, G *et al.* (2008). Adeno-associated virus (AAV) serotype 9 provides global cardiac gene transfer superior to AAV1, AAV6, AAV7, and AAV8 in the mouse and rat. *Hum Gene Ther* **19**: 1359–1368.
16. Maguire, CA, Crommentuijn, MH, Mu, D, Hudry, E, Serrano-Pozo, A, Hyman, BT *et al.* (2013). Mouse gender influences brain transduction by intravascularly administered AAV9. *Mol Ther* **21**: 1470–1471.
17. Foust, KD, Nurre, E, Montgomery, CL, Hernandez, A, Chan, CM and Kaspar, BK (2009). Intravascular AAV9 preferentially targets neonatal neurons and adult astrocytes. *Nat Biotechnol* **27**: 59–65.
18. Gray, SJ, Matagne, V, Bachaboina, L, Yadav, S, Ojeda, SR and Samulski, RJ (2011). Preclinical differences of intravascular AAV9 delivery to neurons and glia: a comparative study of adult mice and nonhuman primates. *Mol Ther* **19**: 1058–1069.
19. Shen, F, Mao, L, Zhu, W, Lawton, MT, Pechan, P, Colosi, P *et al.* (2015). Inhibition of pathological brain angiogenesis through systemic delivery of AAV vector expressing soluble FLT1. *Gene Ther* **22**: 893–900.
20. Vandendriessche, T, Thorrez, L, Acosta-Sanchez, A, Petrus, I, Wang, L, Ma, L *et al.* (2007). Efficacy and safety of adeno-associated viral vectors based on serotype 8 and 9 vs. lentiviral vectors for hemophilia B gene therapy. *J Thromb Haemost* **5**: 16–24.
21. Zincarelli, C, Soltys, S, Rengo, G and Rabinowitz, JE (2008). Analysis of AAV serotypes 1-9 mediated gene expression and tropism in mice after systemic injection. *Mol Ther* **16**: 1073–1080.
22. Schmechel, D, Marangos, PJ, Zis, AP, Brightman, M and Goodwin, FK (1978). Brain endolases as specific markers of neuronal and glial cells. *Science* **199**: 313–315.
23. Tenenbaum, L, Chtarto, A, Lehtonen, E, Velu, T, Brotchi, J and Levivier, M (2004). Recombinant AAV-mediated gene delivery to the central nervous system. *J Gene Med* **6 Suppl 1**: S212–S222.
24. Wakimoto, H, Kesari, S, Farrell, CJ, Curry, WT Jr, Zaupa, C, Aghi, M *et al.* (2009). Human glioblastoma-derived cancer stem cells: establishment of invasive glioma models and treatment with oncolytic herpes simplex virus vectors. *Cancer Res* **69**: 3472–3481.
25. Xiang, H, Nguyen, CB, Kelley, SK, Dybdal, N and Escandón, E (2004). Tissue distribution, stability, and pharmacokinetics of Apo2 ligand/tumor necrosis factor-related apoptosis-inducing ligand in human colon carcinoma COLO205 tumor-bearing nude mice. *Drug Metab Dispos* **32**: 1230–1238.
26. Duiker, EW, Dijkers, EC, Lambers Heerspink, H, de Jong, S, van der Zee, AG, Jager, PL *et al.* (2012). Development of a radioiodinated apoptosis-inducing ligand, rhTRAIL, and a radiolabelled agonist TRAIL receptor antibody for clinical imaging studies. *Br J Pharmacol* **165**: 2203–2212.
27. Jiang, M, Liu, Z, Xiang, Y, Ma, H, Liu, S, Liu, Y *et al.* (2011). Synergistic antitumor effect of AAV-mediated TRAIL expression combined with cisplatin on head and neck squamous cell carcinoma. *BMC Cancer* **11**: 54.
28. Mohr, A, Henderson, G, Dudus, L, Herr, I, Kuerschner, T, Debatin, KM, *et al.* (2004). AAV-encoded expression of TRAIL in experimental human colorectal cancer leads to tumor regression. *Gene Ther* **11**: 534–543.
29. Shi, J, Zheng, D, Liu, Y, Sham, MH, Tam, P, Farzaneh, F *et al.* (2005). Overexpression of soluble TRAIL induces apoptosis in human lung adenocarcinoma and inhibits growth of tumor xenografts in nude mice. *Cancer Res* **65**: 1687–1692.
30. Zhang, Y, Ma, H, Zhang, J, Liu, S, Liu, Y and Zheng, D (2008). AAV-mediated TRAIL gene expression driven by hTERT promoter suppressed human hepatocellular carcinoma growth in mice. *Life Sci* **82**: 1154–1161.
31. Ma, H, Liu, Y, Liu, S, Xu, R and Zheng, D (2005). Oral adeno-associated virus-sTRAIL gene therapy suppresses human hepatocellular carcinoma growth in mice. *Hepatology* **42**: 1355–1363.
32. Pan, G, Ni, J, Wei, YF, Yu, G, Gentz, R and Dixit, VM (1997). An antagonist decoy receptor and a death domain-containing receptor for TRAIL. *Science* **277**: 815–818.
33. Pan, G, O'Rourke, K, Chinnaiyan, AM, Gentz, R, Ebner, R, Ni, J *et al.* (1997). The receptor for the cytotoxic ligand TRAIL. *Science* **276**: 111–113.
34. Sheridan, JP, Marsters, SA, Pitti, RM, Gurney, A, Skubatch, M, Baldwin, D *et al.* (1997). Control of TRAIL-induced apoptosis by a family of signaling and decoy receptors. *Science* **277**: 818–821.
35. Herzog, RW, Fields, PA, Arruda, VR, Brubaker, JO, Armstrong, E, McClintock, D *et al.* (2002). Influence of vector dose on factor IX-specific T and B cell responses in muscle-directed gene therapy. *Hum Gene Ther* **13**: 1281–1291.
36. Jo, M, Kim, TH, Seol, DW, Esplen, JE, Dorko, K, Billiar, TR *et al.* (2000). Apoptosis induced in normal human hepatocytes by tumor necrosis factor-related apoptosis-inducing ligand. *Nat Med* **6**: 564–567.
37. Mori, E, Thomas, M, Motoki, K, Nakazawa, K, Tahara, T, Tomizuka, K, *et al.* (2004). Human normal hepatocytes are susceptible to apoptosis signal mediated by both TRAIL-R1 and TRAIL-R2. *Cell Death Differ* **11**: 203–207.
38. Smith-Arica, JR, Morelli, AE, Larregina, AT, Smith, J, Lowenstein, PR and Castro, MG (2000). Cell-type-specific and regulatable transgenesis in the adult brain: adenovirus-encoded combined transcriptional targeting and inducible transgene expression. *Mol Ther* **2**: 579–587.
39. Xu, R, Janson, CG, Mastakov, M, Lawlor, P, Young, D, Mouravlev, A *et al.* (2001). Quantitative comparison of expression with adeno-associated virus (AAV-2) brain-specific gene cassettes. *Gene Ther* **8**: 1323–1332.
40. Ahmed, SS, Li, H, Cao, C, Sikoglu, EM, Denninger, AR, Su, Q *et al.* (2013). A single intravenous rAAV injection as late as P20 achieves efficacious and sustained CNS Gene therapy in Canavan mice. *Mol Ther* **21**: 2136–2147.
41. Panner, A, James, CD, Berger, MS and Pieper, RO (2005). mTOR controls FLIPS translation and TRAIL sensitivity in glioblastoma multiforme cells. *Mol Cell Biol* **25**: 8809–8823.
42. Hao, C, Beguinot, F, Condorelli, G, Trencia, A, Van Meir, EG, Yong, VW *et al.* (2001). Induction and intracellular regulation of tumor necrosis factor-related apoptosis-inducing ligand (TRAIL) mediated apotosis in human malignant glioma cells. *Cancer Res* **61**: 1162–1170.
43. Seol, DW (2011). p53-Independent up-regulation of a TRAIL receptor DR5 by proteasome inhibitors: a mechanism for proteasome inhibitor-enhanced TRAIL-induced apoptosis. *Biochem Biophys Res Commun* **416**: 222–225.
44. Badr, CE, Wurdinger, T, Nilsson, J, Niers, JM, Whalen, M, Degterev, A *et al.* (2011). Lanatoside C sensitizes glioblastoma cells to tumor necrosis factor-related apoptosis-inducing ligand and induces an alternative cell death pathway. *Neuro Oncol* **13**: 1213–1224.
45. Jane, EP, Premkumar, DR and Pollack, IF (2011). Bortezomib sensitizes malignant human glioma cells to TRAIL, mediated by inhibition of the NF-{kappa}B signaling pathway. *Mol Cancer Ther* **10**: 198–208.
46. de Wilt, LH, Kroon, J, Jansen, G, de Jong, S, Peters, GJ and Kruyt, FA (2013). Bortezomib and TRAIL: a perfect match for apoptotic elimination of tumour cells? *Crit Rev Oncol Hematol* **85**: 363–372.
47. Nagane, M, Pan, G, Weddle, JJ, Dixit, VM, Cavenee, WK and Huang, HJ (2000). Increased death receptor 5 expression by chemotherapeutic agents in human gliomas causes synergistic cytotoxicity with tumor necrosis factor-related apoptosis-inducing ligand in vitro and in vivo. *Cancer Res* **60**: 847–53.
48. Manno, CS, Pierce, GF, Arruda, VR, Glader, B, Ragni, M, Rasko, JJ *et al.* (2006). Successful transduction of liver in hemophilia by AAV-Factor IX and limitations imposed by the host immune response. *Nat Med* **12**: 342–347.
49. Volkmann, X, Fischer, U, Bahr, MJ, Ott, M, Lehner, F, Macfarlane, M *et al.* (2007). Increased hepatotoxicity of tumor necrosis factor-related apoptosis-inducing ligand in diseased human liver. *Hepatology* **46**: 1498–1508.
50. Maguire, CA, Meijer, DH, LeRoy, SG, Tierney, LA, Broekman, ML, Costa, FF *et al.* (2008). Preventing growth of brain tumors by creating a zone of resistance. *Mol Ther* **16**: 1695–1702.
51. Maguire, CA, Gianni, D, Meijer, DH, Shaket, LA, Wakimoto, H, Rabkin, SD *et al.* (2010). Directed evolution of adeno-associated virus for glioma cell transduction. *J Neurooncol* **96**: 337–347.
52. Wu, X, He, Y, Falo, LD Jr, Hui, KM and Huang, L (2001). Regression of human mammary adenocarcinoma by systemic administration of a recombinant gene encoding the hFlex-TRAIL fusion protein. *Mol Ther* **3**: 368–374.
53. Maguire, CA, Bovenberg, MS, Crommentuijn, MH, Niers, JM, Kerami, M, Teng, J *et al.* (2013). Triple bioluminescence imaging for *in vivo* monitoring of cellular processes. *Mol Ther Nucleic Acids* **2**: e99.
54. Broekman, ML, Comer, LA, Hyman, BT and Sena-Esteves, M (2006). Adeno-associated virus vectors serotyped with AAV8 capsid are more efficient than AAV-1 or -2 serotypes for widespread gene delivery to the neonatal mouse brain. *Neuroscience* **138**: 501–510.

Supplementary Information accompanies this paper on the *Molecular Therapy—Oncolytics* website (http://www.nature.com/mto)